

## **SEISMIC VULNERABILITY MODELS OF PIERS UNDER NEAR- FAULT GROUND MOTIONS**

**CHEN Li-bo<sup>1</sup>, WANG Hua-he<sup>2</sup>, GU Yin<sup>2</sup>**

<sup>1</sup> Civil Engineering College, Fuzhou University  
Xueyuan Road No.2, University Town, Fuzhou City, Fujian Province, China  
e-mail: {lbchen}@fzu.edu.cn

<sup>2</sup> Civil Engineering College, Fuzhou University  
Xueyuan Road No.2, University Town, Fuzhou City, Fujian Province, China  
e-mail: {n140520074, cino} @fzu.edu.cn

**Keywords:** Near-fault Ground Motions, Seismic Vulnerability, Residual Deformation, Incremental Dynamic Analysis, Orthogonal Design.

**Abstract.** *Seismic vulnerability models of typical highway piers under the near-fault ground motions were developed based on the incremental dynamic analysis (IDA) method. On the selection criteria of ground motions determined by the authors, totally 30 near-fault or far-field earthquake records were selected. Totally 36 piers were designed as samples by using the orthogonal experimental design method. Each sample was matched by all of the selected ground motions. The numerical models of the piers were established by using OpenSees, in which the nonlinear time history analyses were carried out by the incremental dynamic analysis method. For estimation of the seismic fragility parameters, three different methods were adopted, including the estimation method based on the multiple-stripe analysis idea, the frequency point regression methods from the Monte Carlo sampling and the two-dimensional probability density function integration. The fragility curves were then built up accordingly. The following results can be obtained from the analysis: I) the probability of collapse is higher under near-fault ground motions whereas lower under the far-field motions, i.e., the other three damage states are more likely to happen, when given the same intensity of ground motions; II) by considering two damage indexes, the median values of the fragility curves decrease sharply compared to those with single damage index, which means the pier damage probability increased. Based on the results, it is found that the use of two damage indexes yields more accurate evaluation for the seismic risks of the pier damage and decision making of the seismic retrofit prioritization.*

## 1 INTRODUCTION

Near-fault ground motions have been a hot research topic in the field of earthquake engineering for their special characteristics in recent years. In particular, the pulse-like near-fault ground motions caused by the forward effect and slip effect have a significant dynamic effect on structures, which lead to severe structural damage [1,2,3]. The seismic responses of bridge piers such as strain, curvature and drift ratio can be further amplified, the residual displacements of piers are also very significant for piers under the near-fault ground motions [4,5,6,7]. Therefore, the damage of piers and its probabilities of occurrence should be studied further to investigate the seismic risk of the bridge system. Seismic vulnerability analysis is an important step in the procedure of seismic risk assessment. The fragility function and the incremental dynamic analysis (IDA) are commonly adopted when researchers analyses the seismic risk [8,9]. Nevertheless, the study of seismic vulnerability models of piers under near-fault ground motions is still in its beginning [10,11]. Besides, previous studies have mostly been conducted for ordinary ground motions by using unique bridge sample in the process of seismic fragility analysis. It's necessary to analyze the seismic vulnerability of piers under near-fault ground motions with respect to the special characteristics of near-fault ground motions and by considering severe damage of piers.

## 2 SEISMIC FRAGILITY MODELS' THEORY OF PIERS

The research object of this paper is to set up the vulnerability models of piers which refer to the probability of exceeding a certain damage state when they are under certain level of ground motions. The vulnerability model is assumed to follow the lognormal distribution in this paper, which is expressed as follows:

$$\text{Fragility} = P[D \geq C | IM] = \Phi \left[ \frac{\ln(IM) - \ln(m)}{\beta} \right] \quad (1)$$

where,  $C$  is the capacity of piers,  $D$  is seismic responses of piers,  $IM$  is the intensity of ground motions,  $m$  and  $\beta$  are the median and logarithmic standard deviations of the seismic fragility models.

### 2.1 Seismic Fragility Models Based on IDA method

The seismic vulnerability analysis of piers is carried out by IDA method in this paper. The specific processes are described as below: the values of the ground motion intensity measure are scaled and the seismic responses are obtained by performing nonlinear time-history, then the damage measures and their limit values are selected and determined respectively, finally different methods are adopted to analyze and obtain the fragility parameters, and these models are included in the estimation method such as that based on the multiple-stripe analysis idea, the frequency point regression methods from the Monte Carlo sampling or the two-dimensional probability density function integration method [12,13,14].

### 2.2 The Definition of Piers' Limit States

According to the literature review, the performance levels and damage states of piers are divided into five types[15].The displacement ductility coefficient  $\mu_\Delta$  and residual displacement drift ratio  $DR$  are commonly selected as the damage indexes and their limit values of damage states are identified respectively[16,17,18]. The specific quantifications of the damage states of piers are listed in the table 1.

Performance level	Damage States	Displacement Ductility Coefficient	Residual Displacement Drift Ratio
Level-I	Non-damage	$\mu_{\Delta} < 1.0$	$DR < 0.1\%$
Level-II	Minor damage	$1.0 \leq \mu_{\Delta} < 1.2$	$0.1\% \leq DR < 1\%$
Level-III	Moderate damage	$1.2 \leq \mu_{\Delta} < 1.76$	$1\% \leq DR < 1.5\%$
Level-IV	Major damage	$1.76 \leq \mu_{\Delta} < 4.76$	$1.5\% \leq DR < 1.75\%$
Level-V	Collapse	$\mu_{\Delta} \geq 4.76$	$DR \geq 1.75\%$

Table 1: Limit states of piers

### 3 PIER SAMPLES AND NONLINEAR FINITE ELEMENT ANALYSIS

#### 3.1 Design of Pier Samples

With reference to the existing design codes of China and the literature material, pier samples are designed by orthogonal test method in this paper[19,20]. The specific information of pier samples is listed in the table 2.

Number of Level	Designed Parameters	The Value of Designed Parameters		
3	Slenderness Ratio	4	7	10
	Axial Load Ratio	6%	12%	18%
	Reinforcement Ratio	1.0%	1.6%	2.2%
	Stirrup Ratio	0.4%	0.8%	1.2%
	Pier's Diameter(m)	1.2	1.6	2.0
2	Strength Grades of Concrete	C30		C35
	Strength Grades of Longitudinal	HRB400		HRB335
	Strength Grades of Stirrup	HRB335		HPB300

Table 2: Selected parameters and its values of piers

According to the level of the designed parameters as well as the mixed level orthogonal design test table, the mixed level design test table  $L_{36}(2^3 \times 3^5)$  is selected and 36 pier samples are obtained in this paper.

#### 3.2 Nonlinear Finite Element Pier Models

Finite element analytical models of piers are built by using the OpenSees software[21]. The specific modeling details are shown as below: Force-based beam-column element is adopted to simulate piers. Piers are considered to be made up of fiber element. Concrete01 WithSITC material is selected as the concrete constitutive model of pier and consequently the residual displacement could be captured more accurately [22]. Steel02 material is elected as piers' steel constitutive model. Rayleigh damping mode is chosen and the adopted damping ratio is 3%[23]. The connection between the pier and foundation is rigid linked directly.

#### 3.3 The Input of Ground Motions

The input of ground motions are selected from PEER Strong Motion Database. According to the relevant literature, the selection criteria of earthquakes are determined and listed in the table 3[24].

The Type of Earthquakes	Type	Distance to Fault	Magnitude	PGV/PGA
Near-fault Ground Motions	Pluse-like	0~20km	6~8	>0.15s
Far-field Ground Motions	Ordinary	20~100km	6~8	≤0.15s

Table 3: Selected criteria of ground motions

Totally 30 near-fault or far-field ground motions are selected based on the aforementioned criteria. In order to simulate the seismic response of piers more accurately, three-directional ground motion input is taken in this paper. Simultaneously, PGV is selected to be the intensity measure[25]. Moreover, the selected ground motions are truncated because the original durations are too long.

#### 4 SEISMIC FRAGILITY ANALYSIS OF PIERS

Thirty-six pier samples are matched by all of the selected ground motions in this section. The seismic responses of piers are obtained by IDA method and analyzed by different methods, the seismic fragility models and their parameters are got by different mathematical statistics method.

##### 4.1 The Estimation Method Based on the Multiple-Stripe Analysis Idea

Multiple-stripe analysis is an alternative nonlinear dynamic analysis method. It is mainly for performing the nonlinear time history analysis by a series of ground motions scaled to specific levels. The principle of the method is used as reference in this paper and the concrete steps are as follows. The pier damage states are calculated based on the seismic responses of piers that are obtained from the IDA method. Then, the likelihood function is assumed to follow the binomial distribution. Finally, the fragility parameters and corresponding curves are acquired by the maximum likelihood method [12].

In the process of fragility analysis, the likelihood function is assumed to follow the binomial distribution which is expressed as follows:

$$\text{Likelihood} = C_n^j p^j (1-p)^{n-j} \quad (2)$$

where,  $n$  is the number of pier samples,  $j$  is the number of piers that are in a certain damage state,  $p$  is the probability of damage that can be calculated from equation (1).

The specific calculated equation of the likelihood function can be got by equation (1) and equation (2), which is shown as below:

$$\text{Likelihood} = \prod_{i=1}^m C_n^j \Phi \left( \frac{\ln(IM_i) - \ln(\theta)}{\beta} \right)^j \times \left( 1 - \Phi \left( \frac{\ln(IM_i) - \ln(\theta)}{\beta} \right) \right)^{n-j} \quad (3)$$

According to the maximum likelihood method, the parameters of seismic fragility models can be estimated, based on the following equation.

$$\left\{ \hat{\theta}, \hat{\beta} \right\} = \arg \max_{\theta, \beta} \sum_{i=1}^m \left\{ \ln C_n^j + j \ln \Phi \left( \frac{\ln(IM_i/\theta)}{\beta} \right) + (n-j) \ln \left( 1 - \Phi \left( \frac{\ln(IM_i/\theta)}{\beta} \right) \right) \right\} \quad (4)$$

The seismic vulnerability curves obtained by this method are listed in Figure 1.

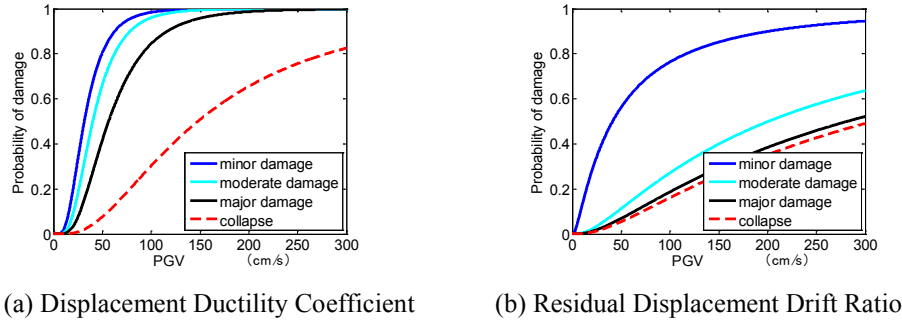


Figure 1: Seismic fragility curves of piers (Near-fault)

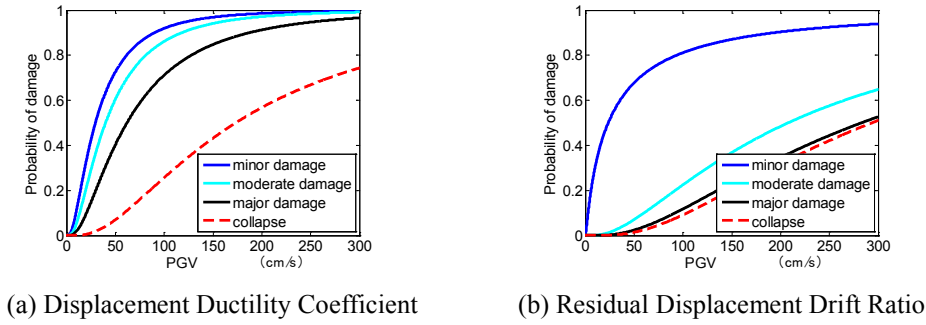


Figure 2: Seismic fragility curves of piers (Far-field)

#### 4.2 The Frequency Point Regression Methods from the Monte Carlo Sampling

The seismic responses of piers under the selected ground motions are firstly recorded in this method and the damage states of piers are evaluated by the responses. Then the number of piers in four types of damage states is counted and divided by the total number of piers to get the corresponding damage probability. The Fragility curves and their parameters are got by using the method of the least squares method [13].

The damage probability in this method can be illustrated as follows:

$$p_j = \frac{\left( \sum_{i=1}^{k \times N} F_i \right)_j}{k \times N} \quad (5)$$

where,  $N$  is the number of pier samples,  $k$  is the number of selected ground motions and  $k$  is equal to 30,  $F_i$  is the limit state function of piers and its values are below:

$$F_i = \begin{cases} 0, & D^i < C^i \\ 1, & D^i \geq C^i \end{cases} \quad (6)$$

According to equation (1) and equation (5), the deviation between the two equations can be illustrated by,

$$\sum_{j=1}^M \delta_j^2 = \sum_{j=1}^M \left[ \frac{\left( \sum_{i=1}^{k \times N} F_i \right)_j}{k \times N} - \Phi \left[ \frac{\ln(IM_j) - \ln(m)}{\beta} \right] \right]^2 \quad (7)$$

In order to obtain the parameters of the fragility models, the least squares method is adopted to minimize the deviation, the values are as below:

$$\left\{ \hat{\theta}, \hat{\beta} \right\} = \arg \min_{\theta, \beta} \sum_{j=1}^M \left[ \frac{\left( \sum_{i=1}^{k \times N} F_i \right)_j}{k \times N} - \Phi \left[ \frac{\ln(IM_j) - \ln(m)}{\beta} \right] \right]^2 \quad (8)$$

The seismic fragility curves obtained by this method are listed in the following figure.

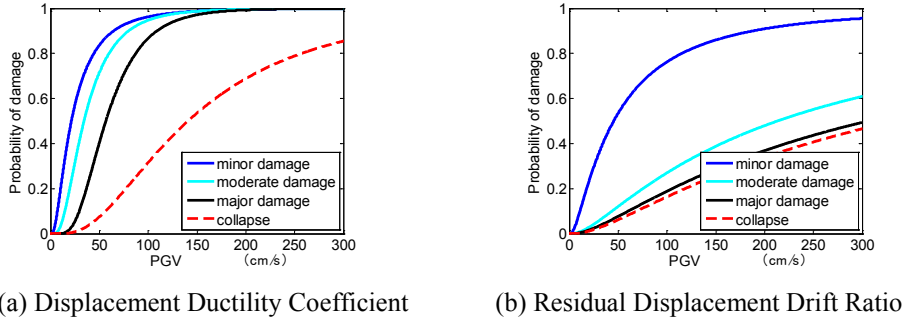


Figure 3: Seismic fragility curves of piers (Near-fault)

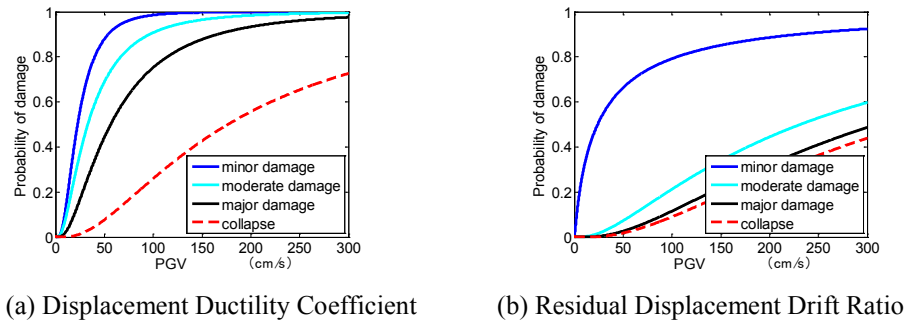


Figure 4: Seismic fragility curves of piers (Far-field)

#### 4.3 The Frequency Point Regression Methods from the Monte Carlo Sampling

The damage index of piers is assumed to yield a certain distribution function in this method, which is assumed to follow the logarithmic normal distribution function in this paper. Given the defined performance level of piers as well as their damage limit states, the damage probability of exceedance can be obtained by integrating the region that is made up of the damage limit states. Furtherly the fragility curves and their parameters are obtained by the least squares method[14]. This method mentioned in this section is mainly under the condition of two damage indexes.

The logarithmic normal distribution function in this method is shown as follows:

$$f(x, y) = \frac{1}{2\pi xy\xi_x\xi_y\sqrt{1-\rho^2}} \exp\left(-\frac{q}{2}\right) \quad (9)$$

$$q = \frac{1}{1-\rho^2} \left[ \left( \frac{\ln x - \lambda_x}{\xi_x} \right)^2 - \frac{2\rho(\ln x - \lambda_x)(\ln y - \lambda_y)}{\xi_x\xi_y} + \left( \frac{\ln y - \lambda_y}{\xi_y} \right)^2 \right]$$

Where,  $\lambda_x$ ,  $\lambda_y$ ,  $\xi_x$  and  $\xi_y$  are the location and scale parameters of the marginal PDF of  $X$  and  $Y$ , respectively.  $X$  and  $Y$  are the selected damage indexes. The parameter  $\rho$  forms a linear correlation coefficient between the two variables.

Each integrated region is composed of the displacement ductility coefficient and the residual displacement drift ratio, the probability is illustrated as follows:

$$PL(x_i, y_i) = \iint_S f(x, y) dS \quad (10)$$

The probability of exceeding a certain damage state can be got by the equation (10), which is shown in equation (11):

$$P = \int_0^{y_i} \int_{x_i}^{\infty} f(x, y) dx dy + \int_{x_i}^{\infty} \int_{y_i}^{\infty} f(x, y) dx dy + \int_{x_i}^{\infty} \int_{y_i}^{\infty} f(x, y) dx dy \quad (11)$$

Furtherly, the equation (11) can be thought to be composed of three parts, which are illustrated below.

$$A = \int_0^{y_i} \int_{x_i}^{\infty} f(x, y) dx dy, B = \int_0^{x_i} \int_{y_i}^{\infty} f(x, y) dx dy, C = \int_{x_i}^{\infty} \int_{y_i}^{\infty} f(x, y) dx dy \quad (12)$$

Where region A is mainly controlled by the displacement ductility coefficient, region B is controlled by the residual displacement drift ratio and region C is controlled by the two damage indexes. The probability density surface and its corresponding integrated region are listed for better illustration of each damaged region, which are shown in the following figure.

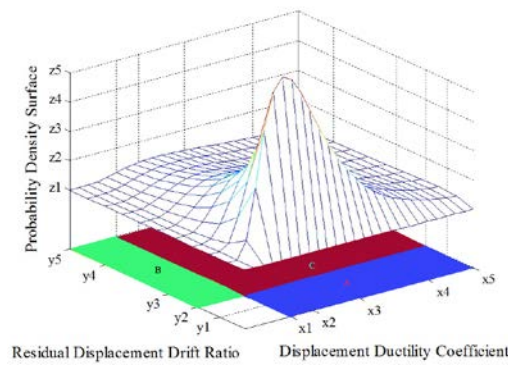


Figure 5: Probability density surface and its integrated range

The contribution of different regions to each damage state of piers is shown in the form of histogram. As the trend that the pier under the near-fault ground motions and far-field ground motions is almost the same, piers under the near-fault ground motions are taken as an example in this paper, which are illustrated in Figure 6.

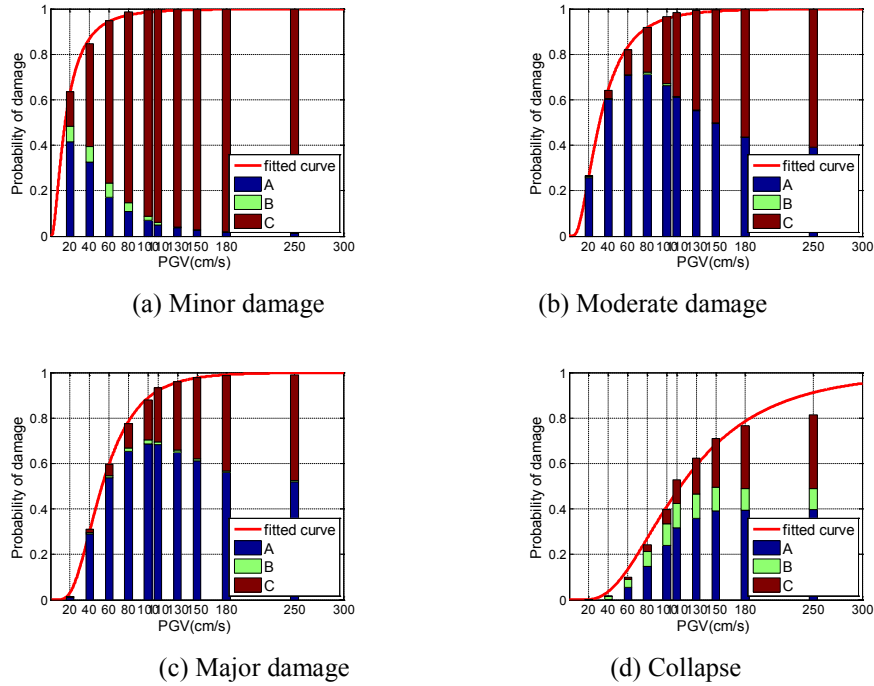


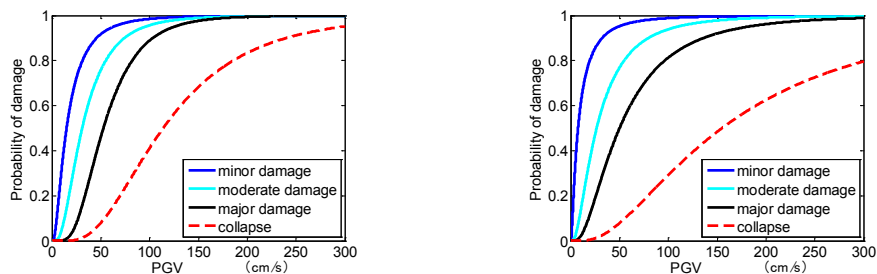
Figure 6: Seismic fragility curves and proportion of each part (near-fault ground motions)

The following results can be obtained from the above figure. The displacement ductility coefficient and the residual displacement drift ratio both play a major role in the condition that piers are in in the case of minor damage state. The displacement ductility coefficient is important in the circumstance where piers are in the other three damage states. However, the importance of residual displacement drift ratio doesn't stand out when piers are in the Minor damage state and Moderate damage as well as Major damage, yet when piers are in the Collapsed damage state, its significance improves greatly. Therefore, when piers are under the near-fault ground motions, the residual displacement of piers isn't negligible and it is necessary to consider both the ductility coefficient and the residual displacement in the analysis of seismic risk.

Similarly, the deviations between equation (1) and the equation (11) can be acquired and according to the east squares method, the parameters can be obtained and be illustrated in the equation (13).

$$\left\{ \hat{\theta}, \hat{\beta} \right\} = \arg \min_{\theta, \beta} \sum_{j=1}^N \left[ \left( 1 - \iint_S f(x, y) dS \right)_j - \Phi \left[ \frac{\ln(IM_j) - \ln(m)}{\beta} \right] \right]^2 \quad (13)$$

The seismic vulnerability curves of piers are acquired under the circumstances with both the displacement ductility coefficient and the residual displacement drift ratio, which are shown as follows.





(a) Near-fault

(b) Far-field

Figure 7: Seismic fragility curves of piers

The seismic vulnerability analysis of piers is carried out according to the three methods previously presented in this paper and the corresponding seismic fragility parameters are obtained. In order to facilitate the analysis, the three analysis methods are denoted Method 1 Method 2 and Method 3, respectively. The specific summary is presented in the following table 4 and table 5.

Method	Damage	Minor damage		Moderate damage		Major damage		Collapsed	
	Index	$m$	$\beta$	$m$	$\beta$	$m$	$\beta$	$m$	$\beta$
1	$\mu_{\Delta}$	31.51	0.54	40.24	0.52	56.41	0.57	145.05	0.76
	$DR$	41.26	1.24	201.09	1.14	281.69	1.16	308.10	1.13
2	$\mu_{\Delta}$	27.25	0.50	37.22	0.48	56.72	0.51	151.24	0.71
	$DR$	45.43	1.11	213.47	1.23	306.01	1.26	334.15	1.23
3	$\mu_{\Delta} + DR$	15.00	0.87	31.01	0.68	52.74	0.53	113.89	0.58

Table 4 Fragility parameters of piers (near-fault ground motions)

Method	Damage	Minor damage		Moderate damage		Major damage		Collapsed	
	Index	$m$	$\beta$	$m$	$\beta$	$m$	$\beta$	$m$	$\beta$
1	$\mu_{\Delta}$	29.61	0.87	39.97	0.85	61.84	0.86	173.53	0.84
	$DR$	23.51	1.64	207.99	0.96	283.10	0.87	293.85	0.81
2	$\mu_{\Delta}$	22.88	0.89	33.09	0.84	56.41	0.84	176.75	0.88
	$DR$	23.89	1.76	231.74	1.05	309.57	0.94	345.72	0.92
3	$\mu_{\Delta} + DR$	7.51	1.14	26.58	0.86	49.98	0.78	155.19	0.79

Table 5 Fragility parameters of piers (far-fault ground motions)

The following results can be obtained from Table 4 and Table 5:

1) Given the same intensity and the analyzed method 3, the probability of collapse is higher under near-fault ground motions, whereas the probability of damage is lower when piers are in the other three damage states. When it comes to the far-field ground motions, damage states of piers are just of the contrary tendency.

2) Considering the single damage index, the fragility parameters acquired by method 1 and method 2 approximates and they deviate slightly. The main reason for the deviation is due to their own limitations of the mathematical statistics methods used in the analysis. The deviations of the parameters decrease when the number of the considered ground motions and pier samples increase.

3) The median values of the seismic vulnerability curves obtained by Method 3 are lower than those obtained by Method 1 and Method 2. The reason for the decrease is due to the effect of residual displacements. The decrease of the median value also indicates that the damage probability of piers under the same ground motion can further increase.

## 5 CONCLUSIONS

The piers which serve as the main components of bridges usually suffer more serious damage than other components under the near-fault ground motions. Therefore, it is of great importance theoretically and practically to analyze the seismic vulnerability of the piers under near-fault ground motions. Based on the results, the suggestions on the seismic evaluation and seismic retrofit prioritization can be furtherly provided. The seismic vulnerability models of piers under near-fault ground motions are studied in this paper, the main research conclusions are as follows:

- From analyzing the effect of near-fault or far-field ground motions on the seismic vulnerability of piers, the following results can be obtained: when the double damage indexes are considered, the probability of collapse is higher under near-fault ground motions whereas the probability of the other three damage states is higher under the far-field motions when given the same intensity of ground motions. Therefore, the effect of near-fault ground motions should be taken into account in the subsequent analysis of the seismic risk assessment of the structure.
- With respect to the proportion of probability of piers under each damage state, the following conclusions can be drawn: (1) The contribution of the displacement ductility coefficient to the damaged probability that piers under near-fault ground motions are in four damage states is prominent. (2) The contribution of the residual displacement of the pier is mirror in the case of the condition that piers are in the first three damage states whereas its contribution increases sharply when piers are collapsed. Therefore, the residual displacement of the pier under the near-fault ground motions can't be ignored in the process of vulnerability assessment
- By comparison on the seismic fragility models acquired by different methods, it is indicated that: Considering the two damage indexes, the median values of seismic vulnerability models obtained by the two-dimensional probability density function integration method decrease compared to that of considering a single damage index. With the decrease of median value, the damage probability of pier increases correspondingly. Therefore, the seismic risk of the pier can be more accurately assessed under the consideration of two damage indexes.

## REFERENCES

- [1] Abrahamson N A, Somerville P G. Effects of rupture directivity on probabilistic seismic hazard analysis [C]. Proceedings of the 6th International Conference on Seismic Zonation, Earthquake Engineering Research Institute, Palm Spring, 2000.
- [2] Bray J D, Marek R A. Characterization of forward-directivity ground motions in the near-fault region [J]. Soil Dynamics and Earthquake Engineering, 2004, 24(11):815-828.
- [3] Somerville P G, Smith N F, Graves R W. Modification of empirical strong ground attenuation relations to include the amplitude and duration effects of rupture directivity [J]. Seismological Research Letters, 1997, 68(10):199-222.
- [4] Phan V, Saiidi M S, Anderson J, Ghasemi H. Near-fault ground motion effects on reinforced concrete bridge columns [J]. Journal of Structural Engineering, 2007, 133(7): 982-989.

- [5] Kunnath S K, Erduran E, Chai Y, Yashinsky M. Effect of near-fault vertical ground motions on seismic response of highway overcrossings [J]. *Journal of Bridge Engineering*, 2008, 13(3): 282-290.
- [6] Brown A, Saiidi M S. Investigation of effect of near-fault motions on substandard bridge structures [J]. *Earthquake Engineering and Engineering Vibration*, 2011, 10(1): 1-11.
- [7] Choi H H, Saiidi M S. An Exploratory Experimental Study of Near-fault Ground Motion Effects on Reinforced Concrete Bridge Columns [J]. *American Concrete Institute Structural Journal*, 2010, 107(1):3-12.
- [8] Shinozuka M, Feng M Q, Kim H, Kim S. Nonlinear Static Procedure for Fragility curve Development [J]. *Journal of Engineering Mechanics*, 2000, 126(12): 1287–1295.
- [9] Nielson B G, DesRoches R. Analytical seismic fragility curves for typical bridges in the central and southeastern United States [J]. *Earthquake Spectra*, 2007, 23(3): 615-633.
- [10] Psycharis I N, Fragiadakis M, Stefanou I. Seismic reliability assessment of classical columns subjected to near-fault ground motions. [J]. *Earthquake engineering & structural dynamics*, 2013, 42(14): 2061-2079.
- [11] Billah A M, Alam S. Seismic performance evaluation of multi-column bridge bents retrofitted with different alternatives using incremental dynamic analysis [J]. *Engineering Structures*, 2014, 62–63(3):105-117.
- [12] Baker J W. Efficient Analytical Fragility Function Fitting Using Dynamic Structural Analysis [J]. *Earthquake Spectra*, 2015, 31(1):579-599.
- [13] Chen Libo, Wang Jiajia, Shangguan Ping. Research of seismic vulnerability model for skew highway girder bridges. *Engineering Mechanics*. (in Chinese, accepted)
- [14] Uma S R, Stefano Pampanin, Constantin Christopoulos. Development of Probabilistic Framework for Performance-Based Seismic Assessment of Structures Considering Residual Deformations [J]. *Earthquake Engineering*, 2010, 14(7):1092-1111.
- [15] HAZUS-MH. Earthquake model technical manual [M]. Washington, D C: Federal Emergency Management Agency. 2003.
- [16] Hwang H, Liu J, Chiu Y. Seismic fragility analysis of highway bridges [R]. Memphis, T N. Center for Earthquake Research and Information, the University of Memphis, 2001.
- [17] Japan Road Association. Design specifications of highway bridges. Part V:Seismic design [S]. Tokyo, Japan, 2012.
- [18] Li Yu. Research on Performance-based Seismic Design and Evaluation for Bridge Structures Considering Residual Displacement and Soil-structure Interaction Effects [D]. Beijing Jiaotong University,2010.
- [19] JTG/T B02-01-2008. Guideline for seismic design for highway bridges [S]. Beijing: China Communications Press, 2008.
- [20] Li Gui-qian. Experimental Study and Numerical Analysis on Seismic Performance of Reinforced Concrete Bridge Columns [D].Chong Qing Jiaotong University ,2010.
- [21] Mazzoni S, McKenna F, Fenves G L. OpenSees command language manual [M]. Pacific Earthquake Engineering Research Center. Berkeley, CA. 2005.

- [22] Won K L. Simulation and Performance-based Earthquake Engineering Assessment of Self-centering Posttensioned Concrete Bridge Systems [D]. Stanford University, 2007.
- [23] Hsu K T, Cheng C C, Yu C P, et al. Evaluation of the Dynamic Characteristics of an Extradosed Bridge Using Microwave Interferometer[J]. *Advanced Materials Research*, 2011,374(377):2426-2429.
- [24] Qiao Min-yuan. Research on Bridge Seismic Responses Under the Excitation of Near-fault Ground Motions [D]. Beijing Jiaotong University ,2013.
- [25] Akkar S, Özen Ö. Effect of peak ground velocity on deformation demands for SDOF systems [J]. *Earthquake Engineering & Structural Dynamics*, 2005, 34(13):1551–1571.